[11] Rai T, Dantes P, Bahreyni B, Kim WS. A stretchable RF antenna with silver nanowires. *IEEE Electron Device Lett.* 2013; 34(4):544–546.

[12] Pierantoni L, Dragoman M, Mencarelli D. Analysis of a microwave graphene-based patch antenna. Paper presented at: European Microwave Conference (EuMC); 2013:381–383.

[13] Zhu W, Farmer DB, Jenkins KA, et al. Graphene radio frequency devices on flexible substrate. *Appl Phys Lett.* 2013;102 (23):233102.

[14] Graphene supermarket.

[15] Bayram Y, Zhou Y, Shim BS, et al. E-textile conductors and polymer composites for conformal lightweight antennas. *IEEE Trans Antennas Propag.* 2010;58(8):2732–2736.

How to cite this article: Elmobarak HA, Rahim SKA, Abedian M, Soh PJ, Vandenbosch GAE, Lo YC. Assessment of multilayered graphene technology for flexible antennas at microwave frequencies. *Microw Opt Technol Lett*. 2017;59:2604–2610. https://doi.org/10.1002/mop.30783

Received: 26 March 2017

DOI: 10.1002/mop.30782

Suspended individual SWCNT characterization via bottom gate FET configuration

Mingguang Tuo[1] | Lu Wang[1] | Moh R. Amer[2,3] | Xiaoju Yu[1] | Stephen B. Cronin[4] | Hao Xin[1]

[1] Department of Electrical and Computer Engineering, University of Arizona, Tucson, Arizona 85721

[2] Department of Electrical Engineering, University of California, Los Angeles, Los Angeles, California 90095

[3] Center of Excellence for Green Nanotechnologies, King Abdulaziz City for Science and Technology, Riyadh 11442, Saudi Arabia

[4] Department of Electrical Engineering, University of Southern California, Los Angeles, California 90089

Correspondence
Mingguang Tuo, University of Arizona, Electrical and Computer Engineering, Tucson, Arizona, United States.
Email: tuo@email.arizona.edu

Abstract

The microwave transmission properties of suspended, quasi-metallic individual single-walled carbon nanotubes (SWCNTs) with a bottom gate field-effect transistor (FET) configuration have been investigated up to 10 GHz by standard two-port *S*-parameter measurements under different gate bias voltages. A tapered coplanar waveguide (CPW) transmission-line test fixture is designed to overcome the parasitic and mismatch issues. An open-through de-embedding algorithm has been applied to extract the intrinsic properties of SWCNTs. And an equivalent circuit model has been proposed to fit the extracted measurement data as a function of the bottom gate bias voltage, facilitating the applications of CNTs into high-frequency nanocircuits. Moreover, the properties of our transistor device are found to change after a period of time.

KEYWORDS

bottom gate FET, de-embedding, equivalent circuit model, individual SWCNT, suspended, tapered transmission-line

1 | INTRODUCTION

CARBON nanotubes (CNTs) attracted people's interests since being discovered.[1] Due to their unique electrical properties, they can be considered as potential candidates for nanoscaled electronics. Some applications of CNTs have been demonstrated such as a field-effect transistor (FET) using aligned semiconducting CNT with a cutoff frequency greater than 70 GHz,[2] CNT antennas resonant in the terahertz (THz) regime,[3,4] etc. Microwave properties of CNT ensembles such as mats[5,6] and bundles[7] have been studied as well. Microwave transmission properties of back gate CNT buddle based FET have been characterized up to 12 GHz on a heavily n^+ doped silicon substrate in Ref. [8]. However, potential problems of characterizing the intrinsic microwave properties of individual CNTs still exist, including challenges in high-frequency measurement such as mismatch between high intrinsic CNT impedance (eg, ~10 kΩ to MΩ) and typical microwave measurement systems (eg, 50 Ω), severe parasitic effects and fabrication difficulties. In addition, an indispensable accurate model is needed to further investigate the CNTs potential towards high-frequency applications.

To address these issues and obtain accurate microwave properties of individual CNTs, a CNT-FET configuration with a 2-μm wide bottom gate electrode has been developed, incorporating a tapered coplanar waveguide (CPW) transmission-line test fixture, to extract the intrinsic properties of individual single-walled CNTs (SWCNTs) by measuring the standard two-port *S*-parameters. The suspended SWCNTs are grown in series across a center gap in the CPW signal trace. The two ports of the tapered CPW test fixture (as shown in Figure 1) serve as the drain and source

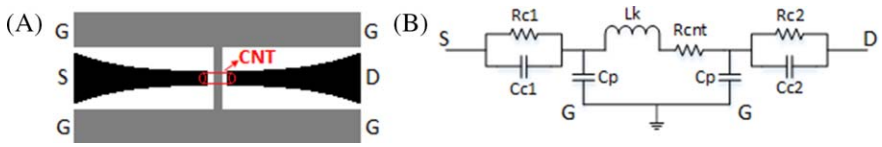

FIGURE 1 (A) The schematic of the CNT-FET structure (top view, not in-scale) and (B) the corresponding equivalent circuit model of the intrinsic SWCNT. [Color figure can be viewed at wileyonlinelibrary.com]

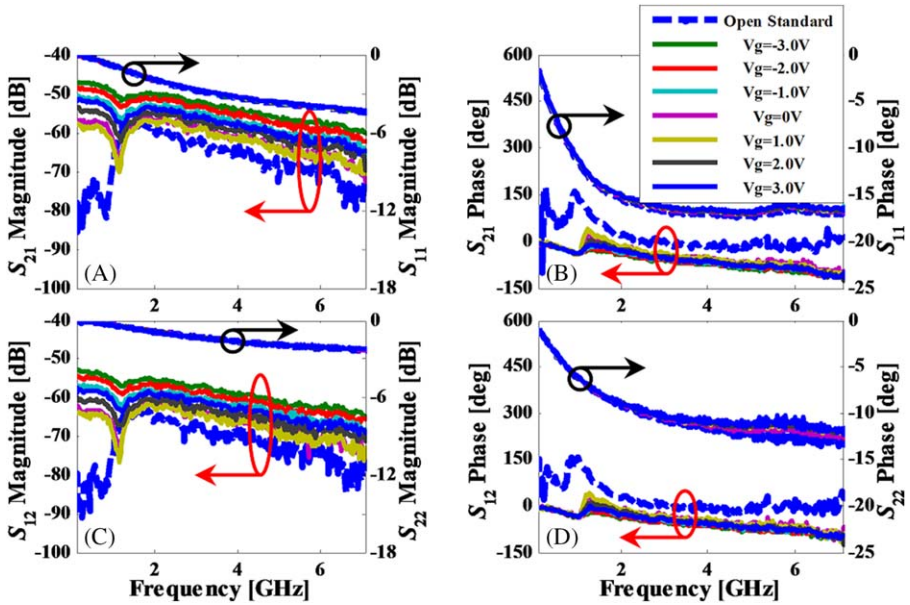

FIGURE 2 Measured *S*-parameters of the SWCNT-FET device under different gate bias voltages as well as those of the "open" standard. [Color figure can be viewed at wileyonlinelibrary.com]

electrodes of the FET. The ground plane of the CPW test fixture connecting to the electrode underneath the suspended CNT serves as the bottom gate electrode of the FET. This tapered test fixture not only improves the matching between the CNT-FET and the measurement system, but also most critically reduces the capacitive coupling between the drain and source electrodes. The detailed device fabrication process is presented in Ref. [9]. Unlike the previously reported CNT-FET structures where CNTs are gone through the lithography process, the suspended samples not only avoid defects induced by the lithography process but also eliminate potential interactions between the nanotube and the substrate, thus enabling characterization of intrinsic properties of pristine, defect-free CNT.

2 | MEASUREMENTS AND PARAMETERS EXTRACTION

The schematic of the CNT-FET structure and the corresponding equivalent circuit model with the three FET electrodes labeled are shown in Figure 1. The detailed layout of the tapered CPW test fixture and a scanning electron microscope (SEM) image of the fabricated device can be found in Ref. [9]. To obtain the microwave transmission properties of the SWCNT devices, an Agilent E8361A vector network analyzer (VNA) along with two 150-μm-pitch ground-signal-ground (GSG) probes (GGB Industries Inc.) are used to implement the standard two-port *S*-parameter measurements

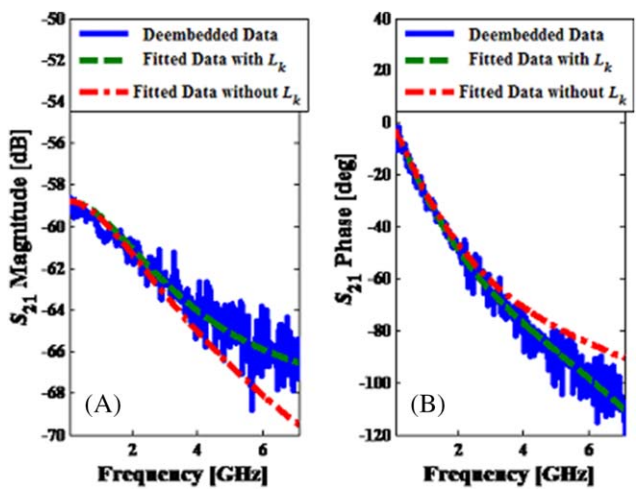

FIGURE 3 Comparison between the de-embedded measured and the equivalent circuit model fitted S_{21} (A) magnitude and (B) phase, both with and without kinetic inductance L_k. [Color figure can be viewed at wileyonlinelibrary.com]

TABLE 1 Fitted Parameter Values in the Equivalent Circuit Under Different Gate Biases (1st Measurement)

V_g (V)	R_{cnt} (kΩ)	L_k (nH)	C_p (fF)	R_{c1} (kΩ)	C_{c1} (fF)	R_{c2} (kΩ)	C_{c2} (fF)
−3.0	3.569	62.993	5.604	12.716	0.002	11.527	0.001
−2.0	3.999	68.706	5.022	19.473	0.003	10.002	0.0013
−1.0	5.521	100.849	3.575	16.014	0.001	22.364	0.0016
0	8.933	250.185	1.859	46.439	0.001	31.259	0.0012
1.0	8.073	295.682	2.009	56.843	0.001	26.419	0.001
2.0	6.214	204.799	2.595	29.578	0.001	25.761	0.0026
3.0	5.051	123.583	3.446	16.64	0.001	26.499	0.0013

under zero drain-to-source bias condition. *S*-parameter measurements of the CNT-FET device up to 7.1 GHz under different gate bias voltages (called 1st measurement) as well as the "open" standard (no nanotube across the center gap) and the "through" standard (continuous signal trace without the center gap) are implemented under the same calibration condition. The measured *S*-parameters magnitude and phase of the CNT-FET under different gate bias voltages (from −3 to +3V with a step of 1V) as well as those of the "open" standard are shown in Figure 2. The measured *S*-parameters of the "open" and "through" standards are used to de-embed the parasitics of the electrodes allowing extraction of the intrinsic property of the SWCNT under test. The detailed information about the de-embedding algorithm can be found in Ref. [9]. Compared to the equivalent circuit model reported in Ref. [10], an additional shunt capacitance C_p which is due to the coupling between the suspended CNT and the bottom gate electrode (not fully eliminated from the de-embedding process) is introduced to obtain a good fit between the measured microwave response and the model. The parameters in the equivalent circuit model of Figure 1b are fitted by using the optimization tool in Advanced System Design (ADS) software package. The optimization algorithm is "Gradient" and the optimization goals are to minimize the S_{21} magnitude and phase differences between the equivalent circuit model and de-embedded test data for the whole frequency range.

In principle, the intrinsic resistance of CNT is given by $h/4e^2 \cdot l_{cnt}/l_{mfp}$ where l_{cnt} is the length of the CNT and l_{mfp} is the mean free path due to the scattering.[11] When the gate bias voltage is applied, l_{mfp} becomes larger and comparable to l_{cnt}. Also, the Fermi-velocity of electrons in the SWCNT increases when the gate bias voltage is applied, which should induce a decrease of the kinetic inductance. The fitted values of the different parameters in the equivalent circuit model in

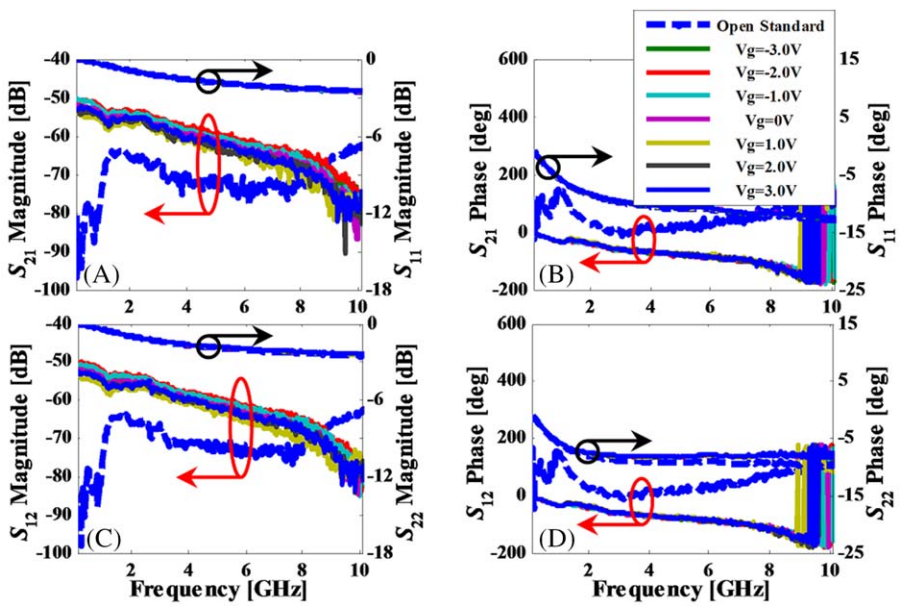

FIGURE 4 Measured (after about a year) *S*-parameters of the SWCNT-FET device under different gate bias voltages as well as those of the "open" standard. [Color figure can be viewed at wileyonlinelibrary.com]

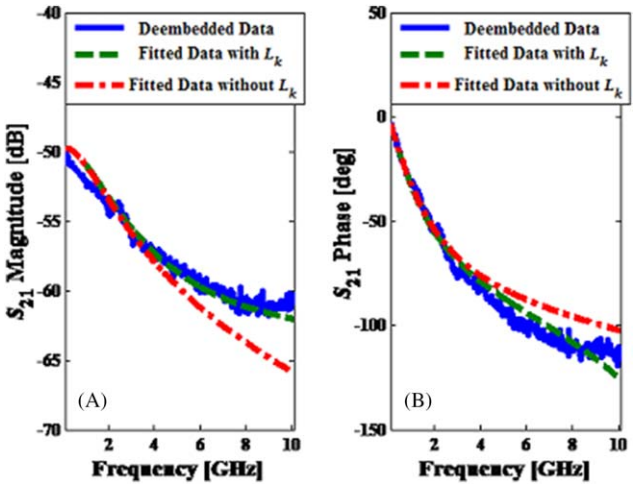

FIGURE 5 Comparison between the de-embedded measured and the equivalent circuit model fitted S_{21} (A) magnitude and (B) phase for the 2nd measurement, both with and without kinetic inductance L_k. [Color figure can be viewed at wileyonlinelibrary.com]

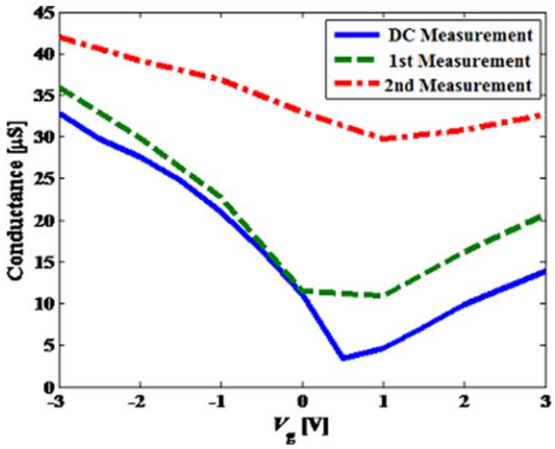

FIGURE 6 DC conductance and RF conductance based on fitted parameters versus gate bias voltage for two sets of measurement. [Color figure can be viewed at wileyonlinelibrary.com]

Figure 1 are listed in Table 1. The comparison of S_{21} magnitude and phase between the equivalent circuit model fitted and the de-embedded measured data at $V_g = 0$ V is shown in Figure 3. Fitted curves without kinetic inductance L_k are plotted in the figures as well. It is seen that with the kinetic inductance, the equivalent circuit model fits quite well to the de-embedded measured data for both S_{21} magnitude and phase. Without the kinetic inductance, the fitted curves show large discrepancy at higher frequencies (ie, greater than 3 GHz). This indicates that the kinetic inductance of the SWCNT has been clearly measured in this work. The fitting curves at all other gate bias voltages result in similar reasonable agreements (not shown).

After about a year, another on-wafer measurement of the same device is done with the same setup but under an independent calibration and the frequency range is also extended up to 10 GHz. It is found that the gate dependence of the device becomes weaker which can be seen from the *S*-parameter measurement results (called 2nd measurement) plotted in Figure 4. To quantify this observation, the 1st measurement has a maximum change of about 11.4 dB while the 2nd measurement just has a maximum change of about 5 dB for S_{21} magnitude for the gate bias voltage range.

Since the measured microwave transmission response of the SWCNT device changes as experimentally observed, the fitted values of each parameter in the equivalent circuit model are different from the 1st measurement as listed in Table 2. It is observed that the resistances become smaller which is consistent with the fact that the measured transmission level is increased. It is also noticed that the fitted kinetic inductance L_k value becomes smaller and its variation for different gate bias voltages becomes smaller compared with the 1st measurement as well. This is consistent with the much smaller differences in the measured S_{21} phase under different gate bias voltages. This difference could be interpreted as the variation of the sample electronic transport properties while exposing the sample in ambient air environment with oxygen absorption.[12,13] The comparison of the S_{21} magnitude and phase between the equivalent circuit model fitted and de-embedded measured data at $V_g = 0$ V (both

TABLE 2 Fitted Parameter Values in the Equivalent Circuit Under Different Gate Biases (2nd Measurement)

V_g (V)	R_{cnt} (kΩ)	L_k (nH)	C_p (fF)	R_{c1} (kΩ)	C_{c1} (fF)	R_{c2} (kΩ)	C_{c2} (fF)
−3.0	1.952	32.002	8.168	9.512	0.001	12.333	0.001
−2.0	1.946	33.799	7.94	8.999	0.001	14.606	0.011
−1.0	1.966	34.297	7.68	8.995	0.001	16.142	0.001
0	2.048	40.503	6.836	11.158	0.001	17.163	0.009
1.0	1.698	36.127	7.809	7.486	0.001	24.471	0.003
2.0	1.629	34.181	8.272	6.933	0.001	23.815	0.001
3.0	1.602	32.092	8.638	6.592	0.001	22.369	0.001

with and without L_k) is shown in Figure 5. With this set of measurement data, it is also observed that without L_k there will be large discrepancy between the equivalent circuit model fitted and the measured results, which further confirms that the kinetic inductance plays an important role in the equivalent circuit model of the intrinsic SWCNT.

The RF conductance (calculated as the reciprocal of the summation of R_{cnt}, R_{c1}, and R_{c2}) for both measurements as a function of the gate bias voltage is plotted in Figure 6. Compared to the DC characterization of the device, it is seen that the fitted RF conductance at zero gate bias from the 1st measurement roughly agrees with the DC conductance, which is about 10 μS. As for the 2nd measurement, the RF conductance at zero gate bias is about 33 μS, which is higher than the DC conductance measured earlier.

3 | CONCLUSION

In conclusion, tapered CPW transmission-line test fixture with reduced parasitic effect and mismatch has been designed to measure the intrinsic microwave properties of suspended and pristine individual SWCNTs. Equivalent circuit model of SWCNT has been utilized to fit the de-embedded measured data. Kinetic inductance of the intrinsic SWCNT is successfully measured. Two sets of microwave measurements performed between about a year interval are compared. Different gate dependences are observed for these two measurements and the difference is attributed to the fact that the CNT-FET device's exposure to oxygen. The equivalent circuit model of individual SWCNT will be useful for future high-frequency nanocircuit applications.

REFERENCES

[1] Iijima S. Helical microtubules of graphitic carbon. *Nature.* 1991; 354:56–58.

[2] Cao Y, Brady GJ, Gui H, Rutherglen C, Arnold MS, Zhou C. Radio frequency transistors using aligned semiconducting carbon nanotubes with current-gain cutoff frequency and maximum oscillation frequency simultaneously greater than 70 GHz. *ACS Nano.* 2016;10:6782–6790.

[3] Hanson GW. Fundamental transmitting properties of carbon nanotube antennas. *IEEE Trans Antennas Propag.* 2005;53: 3426–3435. Nov.

[4] Maksimenkoa SA, Slepvana GY, Nemilentsau AM, Shubaa MV. Carbon nanotube antenna: Far-field, near-field and thermal-noise properties. *Phys E.* 2008;40:2360–2364.

[5] Wang L, Zhou R, Xin H. Microwave (8–50 GHz) characterization of multiwalled carbon nanotube papers using rectangular waveguides. *IEEE Trans Microw Theory Tech.* 2008;56(2):499–506.

[6] Wu Z, Wang L, Peng Y, Young A, Seraphin S, Xin H. Terahertz characterization of multi-walled carbon nanotube films. *J Appl Phys.* 2008;103(9):094324–1–094324–6.

[7] Tselev A, Woodson M, Qian C, Liu J. Microwave impedance spectroscopy of dense carbon nanotube bundles. *Nano Lett.* 2008;8(1):152–156.

[8] ZhangHuo MX, Chan PC, Liang HQ, Tang ZK. Radio-frequency transmission properties of carbon nanotubes in a field-effect transistor configuration. *IEEE Electron Device Lett.* 2006; 27(8):668–670.

[9] Tuo M, Wang L, Amer MR, Yu X, Cronin SB, Xin H. Microwave properties of suspended single-walled carbon nanotubes with a field-effect transistor configuration. *IEEE Int Microw Symp*. Baltimore, MD, 2011.

[10] Plombon JJ, O'brien KP, Gstrein F, Dubin VM, Jiao Y. High-frequency electrical properties of individual and bundled carbon nanotubes. *Appl Phys Lett.* 2007;90:063106–1–063106–3.

[11] Rutherglen C, Burke P. Nanoelectromagnetics: circuit and electromagnetic properties of carbon nanotubes. *Small.* 2009;5: 884–906.

[12] Collins PG, Bradley K, Ishigami M, Zettl A. Extreme oxygen sensitivity of electronic properties of carbon nanotubes. *Science.* 2000;287:1801–1804.

[13] Amer MR, Bushmaker AW, Cronin SB. Anomalous kink behavior in the current-voltage characteristics of suspended carbon nanotubes. *Nano Res.* 2012;5:172–180.

How to cite this article: Tuo M, Wang L, Amer MR, Yu X, Cronin SB, Xin H. Suspended individual SWCNT characterization via bottom gate FET configuration. *Microw Opt Technol Lett*. 2017;59:2610–2614. https://doi.org/10.1002/mop.30782

Received: 27 March 2017

DOI: 10.1002/mop.30781

Compact leaky wave antenna using ferroelectric materials

H. M. Jeon | Z. Ji | Y. Zhuang

Department of Electrical Engineering, Wright State University, Dayton, Ohio

Correspondence
Y. Zhuang, Wright State University, Electrical Engineering, 3640 Colonel Glenn Hwy, Dayton, Ohio, United States 45435.
Email: yan.zhuang@wright.edu

Funding information
Wright State University research challenge award.

Abstract

In this work, we present a leaky wave antenna with an enhanced angular scan rate (ASR) using high permittivity materials. The proto-type leaky wave antenna consists of a